Journal of ELECTRONIC MATERIALS, Vol. 41, No. 1, 2012
DOI: 10.1007/s11664-011-1761-3

A Simple Process for Synthesis of Ag Nanoparticles and Sintering of Conductive Ink for Use in Printed Electronics

INYU JUNG,[1] YUN HWAN JO,[1] INYOUNG KIM,[2] and HYUCK MO LEE[1,3]

1.—Department of Materials Science and Engineering, KAIST, 291 Daehak-Ro, Yusung-Gu, Daejeon 305-701, Republic of Korea. 2.—Research Division of Nano-Mechanical System, Korea Institute of Machinery and Materials, 104 Sinsung-Ro, Yusung-Gu, Daejeon 305-343, Republic of Korea. 3.—e-mail: hmlee@kaist.ac.kr

Various-sized Ag nanoparticles capped with oleylamine were synthesized by means of a thermal decomposition process for low-temperature electronic devices. The Ag nanoparticles, which had diameter of 5.1 nm to 12.2 nm, were synthesized in incubation and ripening stages related to nucleation and growth. After the Ag nanoparticles were made into ink with a proper solvent, inkjet printing and thermal sintering methods were used to form a metal thin film with thickness of 100 nm. A type of thermal sintering related to percolation transformation and surface sintering was conducted at a temperature much lower than the melting point of bulk Ag. The electrical resistivity was examined with the aid of a four-point probe system and compared with the resistivity of bulk Ag, showing that the Ag film had much higher resistivity than bulk Ag. To improve the electrical stability and properties, we applied hexamethyldisilazane (HMDS) surface treatment to the substrate and dipped the as-deposited films into methanol. Both treatments helped to diminish and stabilize the resistivity of the printed conductive films.

Key words: Ag nanoparticles, thermal decomposition, percolation transformation, surface sintering, conductive ink

INTRODUCTION

Inkjet printing technology has recently been investigated to offer an alternative to the conventional vacuum deposition and photolithography used in the printing circuit board industry. In contrast with conventional methods, inkjet printing technology is currently attracting a great deal of attention because of its advantages of being fast, simple, inexpensive, and even providing processability at low temperatures.[1–6] Low-temperature processability is becoming more important on account of developments in plastic electronics, which use plastic substrates that have low glass-transition temperature. One of the most important components of inkjet printing technology is the conductive material. Several candidate conductive materials have been studied, namely molten metal, conductive polymer, and metallic nanoparticle suspension.[7] Of these, the metallic nanoparticle suspension is considered the most promising candidate inkjet printing material. Ink made of metal nanoparticles and a proper solvent can be used at room temperature. It also has better direct-current (DC) conductivity (typically 10^4 S/cm to 10^5 S/cm) than conductive polymer (typically 10 S/cm to 10^2 S/cm).[8]

Nanoparticles made of noble metals such as Au and Ag have been widely studied in terms of their use in inkjet printing material because of their high conductivity, though they also have high melting temperature ($T_{m,Au}$ = 1064°C, $T_{m,Ag}$ = 961°C). Nanoparticles generally exhibit very interesting size-dependent electrical, optical, magnetic, and chemical properties that cannot be achieved with their bulk counterparts.[9] In addition, when their size decreases to the nanoscale, their thermodynamic properties differ significantly from those of

(Received March 16, 2011; accepted September 6, 2011; published online September 17, 2011)

bulk materials. Several groups have reported a size-dependent melting temperature depression in various metallic systems; this behavior enables metal nanoparticles to be sintered at low temperature by means of melting and solidification.[10–14] However, Sivaramakrishnan et al. reported the percolation transformation, which has received attention only recently owing to the importance of the sintering of nanoparticles.[8,15,16] In this type of transformation, the metal nanoparticles lose their ligand shells at a certain temperature, called the percolation temperature, and exhibit conductance through physical contact with each other. The percolation temperature (T_p) is the operationally defined temperature at which the film of metal nanoparticles undergoes an insulator-to-metal transformation.[17] In terms of the percolation temperature, the most important issue in decreasing the sintering temperature is not the size of the nanoparticles but the organic ligand, which melts at a low temperature.[18] Furthermore, using differential scanning calorimetry (DSC), Moon et al.[19] and Kim and Moon[20] observed exothermic peaks of metal nanoparticles during the sintering process.

In this study, we used a simple thermal decomposition process to synthesize various-sized Ag nanoparticles capped with oleylamine. We then applied incubation and ripening stages so that the nanoparticles were synthesized with higher yield and narrower size distribution.[21] Inkjet printing was used to form thin films, and we examined the electrical properties while varying the sintering temperature. The electrical properties for each sintering temperature are discussed in terms of the surface film morphologies and exothermic heat flow for the isothermal sintering temperature. To improve the electrical properties, we subjected the substrate to hexamethyldisilazane (HMDS) surface treatment[22–24] and dipped the printed patterns in methanol.[25–27] These efforts to improve the synthesis and electrical properties enable us to use the Ag nanoparticle suspension for printed electronics.

EXPERIMENTAL PROCEDURES

Materials Preparation

A simple thermal decomposition process was used to synthesize the Ag nanoparticles without using any common reducing agent. In this sense, the synthesis process of this work can be simple, and a heating mantle with a magnetic stirring system was used for the chemical synthesis. Silver nitrate ($AgNO_3$, Sigma-Aldrich) and oleylamine ($C_{18}H_{37}N$, Sigma-Aldrich) were used as the Ag precursor and surfactant. All the chemicals were used as received without further treatment.

In a typical synthesis, 2.5 g $AgNO_3$ was added to a round flask (250 mL) containing 100 mL oleylamine while being stirred. The size and yield of the nanoparticles vary in relation to the synthetic temperature and time. To attain Ag nanoparticles with higher yield and narrower size distribution, we applied two different stages in the synthetic process: a high-temperature stage (180°C) and a low-temperature stage (150°C) as incubation and ripening stages for nucleation and growth.[21] The low-temperature incubation stage was followed by the high-temperature ripening stage, and the duration of each stage was varied. The product was purified by means of a dispersion–centrifugation process. After the product was cooled down to room temperature, methanol (CH_3OH, Sigma-Aldrich) and toluene (C_7H_8, Sigma-Aldrich) were poured into the suspension, which was then centrifuged at 10,000 rpm for 30 min. The resulting nanoparticles were dispersed with the toluene and methanol in a homogenizer bath (Sonic Dismembrator, Fisher Scientific) and centrifuged several times under the same conditions. The Ag nanoparticles were dried in a vacuum oven at 30°C for 10 h and then dispersed with toluene again. Transmission electron microscopy (TEM, FEI Tecnai G2 F30 operated at 300 kV) was used to measure the average size and distribution. More than 200 Ag nanoparticles were counted.

Conductive Ink and Sintering

Conductive ink was made by dispersing Ag nanoparticles capped by oleylamine in the proper hydrophobic solvent. Surface tension and viscosity are important factors of ink for inkjet printing.[28,29] As summarized in Table I, the viscosities of the potential solvents, hexadecane (HD), tetradecane (TD), and a mixture of both (MTH, 50 wt.% HD plus 50 wt.% TD), were 2.16 cP for pure TD, 3.51 cP for MTH, and 3.85 cP for HD. HD was selected as a promising candidate solvent because it had the highest viscosity.

To investigate the appropriate viscosity of the ink, we used an ARES rheometer (ARES-G2; TA Instruments) at shear rate of 100 s^{-1} under all conditions to measure the viscosity. The surface tension was measured by means of the pendant drop method (Phoenix 150 instrument). The inkjet printer used in this work was optimized for ink in the range of 8 cP to 13 cP and 28 dyn/cm to 36 dyn/cm. The ink containing Ag was dispersed in a homogenizer bath for 30 min. The resulting ink was filtered with a 10-μm nylon mesh to prevent any clogging. Prior to the deposition of the conductive ink, HMDS treatment was performed on a

Table I. Viscosity of solvent

Solvent	Viscosity (cP)
Tetradecane (TD)	2.16
50 wt.% TD + 50 wt.% HD (MTH)	3.51
Hexadecane (HD)	3.85

silicon wafer by using the spin-coating method with speed of 3000 rpm for 60 s. To investigate the electrical properties, we used an inkjet printer (Dimatix DMP-2800, Fujifilm) to form thin films on the silicon wafer in an ambient atmosphere. The capping layer of oleylamine on the metal thin films remained even though the dispersion–centrifugation process was repeated several times. After the thin films were dried at room temperature, the silicon wafer was dipped in methanol to remove the residual capping layer. The effect of the methanol dipping treatment was confirmed with the aid of a thermogravimetry analyzer (TGA-TG209F3). A sintering process was conducted after the methanol dipping treatment at temperatures of 150°C, 200°C, and 250°C, and the sheet resistance was measured with a four-point probe station (CMT-SR1000N). Thermal analysis was also conducted by means of DSC (TA Instruments) during the sintering process under various isothermal temperatures.

RESULTS AND DISCUSSION

Formation of Ag Nanoparticles and Conductive Ink

The yield of Ag nanoparticles was higher than 85% in all the experimental conditions, and different-sized Ag nanoparticles were synthesized, as shown in Fig. 1. Monodispersed Ag nanoparticles with diameter of 5.1 nm ($\sigma \leq 7.5\%$, standard deviation) were obtained at 150°C for 1 h and then at 180°C for 5 min; those with diameter of 8.2 nm ($\sigma \leq 8.2\%$) and 12.2 nm ($\sigma \leq 7.7\%$) were synthesized at 150°C for 5 h and then at 180°C for 5 min and 1 h, respectively. As shown in the inset of Fig. 1a, the selected-area electron diffraction (SAED) pattern exhibited a cubic structure with space group *Fm3m* (225) and lattice constant a of 4.086 Å. The four rings correspond to the lattice planes (111), (200), (220), and (311), which are consistent with the face-centered cubic (fcc) phase of pure Ag. The inset of Fig. 1b shows a high-resolution TEM (HRTEM) image of Ag nanoparticles. The interplanar distance of the fringes is 2.36 Å, which corresponds to the (111) planes of pure Ag with fcc structure. Both SAED and HRTEM results confirm the formation of well-crystalline Ag nanoparticles.

The viscosity of the conductive ink measured at 20°C by changing the amount of Ag nanoparticles in a mixture is shown in Fig. 2a. It increased linearly when the Ag content was less than 20 wt.%, and increased steeply when the Ag content was 30 wt.%. Lee et al.[30] explained that, in general, viscosity is linearly proportional to the solid content at low solid concentration of particles in a colloidal suspension. However, the interaction between these colloids is no longer negligible and the viscosity increases rapidly as the colloidal concentration continues to increase. Figure 2b also shows that the surface tension increased as the solid loading was increased. This behavior is similar to the behavior of viscosity. In view of the optimized viscosity (8 cP to 13 cP) and surface tension (28 dyn/cm to 36 dyn/cm) of the ink that is compatible with the inkjet printer, an amount of 30 wt.% Ag nanoparticles was dispersed in pure HD solvent, resulting in viscosity of 10.47 cP and surface tension of 29.02 dyn/cm of the ink.

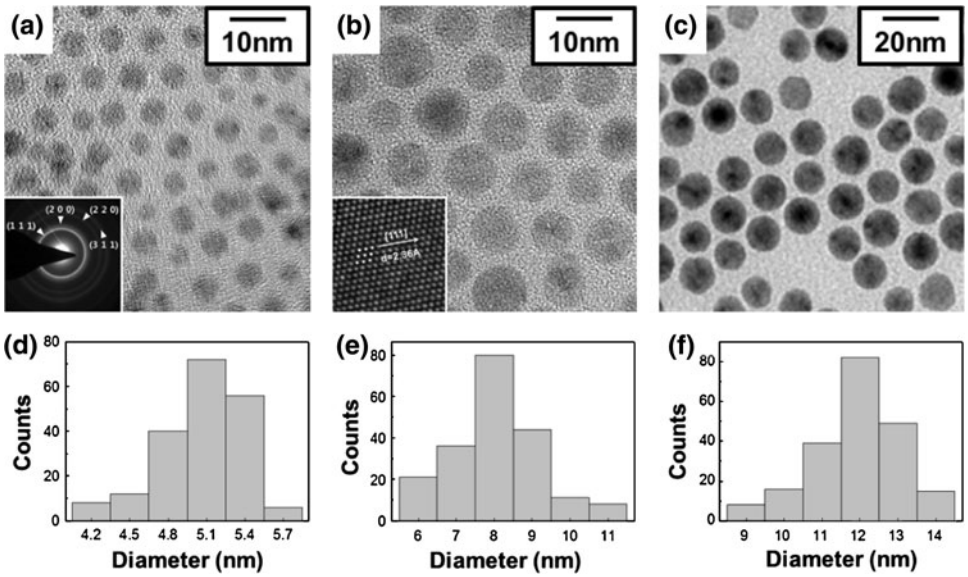

Fig. 1. TEM images of Ag nanoparticles: (a) 5.1 nm nanoparticles ($\sigma \leq 7.5\%$) synthesized at 150°C for 1 h and then at 180°C for 5 min; (b) 8.1 nm nanoparticles ($\sigma \leq 8.2\%$) synthesized at 150°C for 5 h and then at 180°C for 5 min; (c) 12.2 nm nanoparticles ($\sigma \leq 7.7\%$) synthesized at 150°C for 5 h and then at 180°C for 1 h. The inset in (a) shows a typical SAED pattern of Ag crystals. The inset in (b) shows a HRTEM image of Ag crystals. (d–f) Corresponding particle size distribution analyses of Ag nanoparticles obtained under each condition.

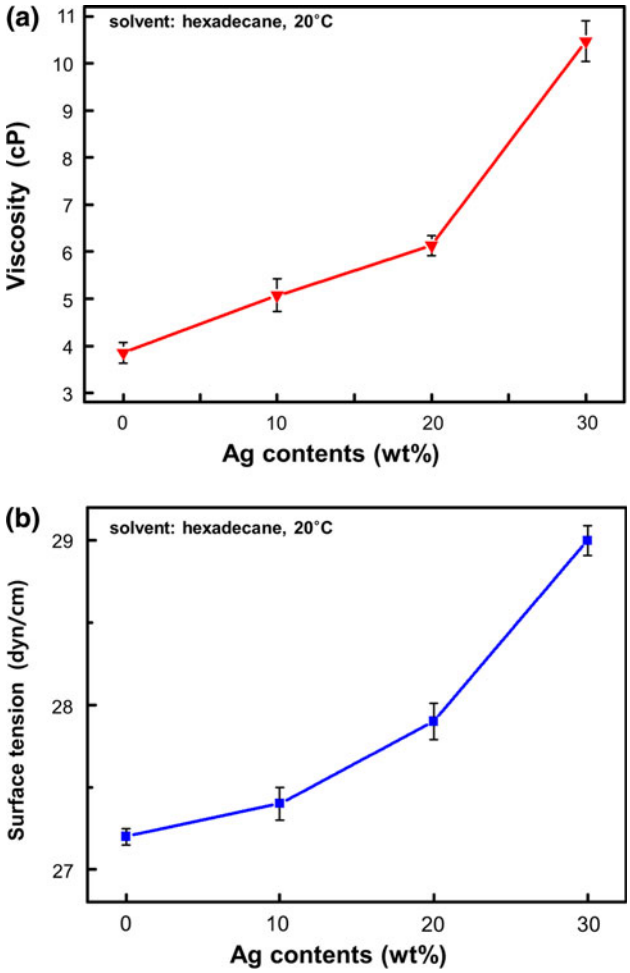

Fig. 2. Conductive ink properties: (a) viscosity and (b) surface tension of Ag ink as a function of Ag content.

Percolation Transformation and Surface Diffusion

It is well known that a size-dependent melting temperature depression can occur in metal nanoparticles, and the melting and solidification at low temperature can lead to the formation of a conductive structure. Recently, however, the percolation transformation has received attention as a possible means of sintering metal nanoparticles.[8,15,16] According to this theory, full melting and solidification are not required. Instead, continuous structure and electrical properties can be found at temperature much lower than the melting temperature because of the elimination of the ligand shells surrounding the metal nanoparticles and subsequent agglomeration induced by the physical contact and coalescence of the nanoparticles.[18] Figure 3 shows the electrical resistivity of conductive films with two different kinds of ink: 5-nm ink with particle diameter of 5.1 nm, and 12-nm ink with particle diameter of 12.2 nm. There are no significant differences at the same sintering temperature, the slight differences being negligible because the error ranges overlap for most of the temperatures. This phenomenon confirms that the percolation transformation is not a result of the size-dependent melting temperature depression.

In addition, surface sintering can affect the coalescence of the nanoparticles and the percolation transformation. The DSC results in Fig. 4 exhibit an exothermic heat flow during the sintering condition for each isothermal temperature. According to the previous reports involving DSC analysis, Moon et al.[19] and Kim and Moon[20] observed exothermic peaks during the sintering of metal nanoparticles and attributed them to surface diffusion of unstable atoms on the nanoparticles. During this reaction, stabilization of the crystal structure, reformation, and reallocation of grain boundaries at the particle interfaces may take place. The atoms on the surface of nanoparticles are generally believed to be very unstable because of higher surface energy, extremely large surface area, and defective structure; that is, surface sintering by means of surface diffusion can occur during thermal sintering at low temperature. Another possible explanation for the exothermic peaks of metal nanoparticles in DSC is the crystallization of amorphous metal nanoparticles or the recrystallization of strained metal nanoparticles on heating. Due to the fact that Ag nanoparticles in this study are well crystalline, as verified in Fig. 1, however, this possibility is eliminated. Furthermore, the fact that the exothermic heat flow intensified as the temperature rose was indicative of the extensiveness of the surface diffusion of nanoparticles. A large, sharp amplitude peak was observed at 250°C, and a small broad peak at 200°C. The peak for the thermal treatment at 150°C was almost negligible in relation to the peaks that occurred at higher temperatures, which implies that the surface sintering and coalescence that occurred at 250°C and 200°C were active, whereas the surface sintering at 150°C was only slight. The surface sintering seems to originate when unstable atoms on the metal nanoparticles undergo surface diffusion and thus large agglomerates may be formed, resulting in enhanced electrical properties. Figure 5a–c shows SEM images of the surface morphology, which indicate that the size of agglomerates become larger with increasing temperature. Although the nanoparticles were barely agglomerated at 150°C, the particles were not isolated or agglomerated well with a continuous structure at 200°C and 250°C. As shown in Fig. 5d, the relation between electrical resistivity and temperature was calculated by measuring the thickness of the printed patterns (100 ± 5 nm).

Electrical Properties

The relation between the electrical properties and the sintering temperature was briefly discussed based on Fig. 3. The well-known hydrophobic surface treatment is HMDS chemical treatment that is

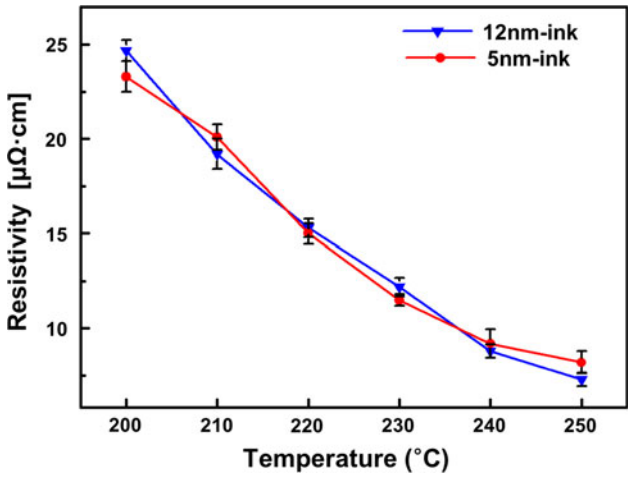

Fig. 3. Electrical resistivity of Ag conductive films made with 5-nm ink and 12-nm ink as a function of sintering temperature.

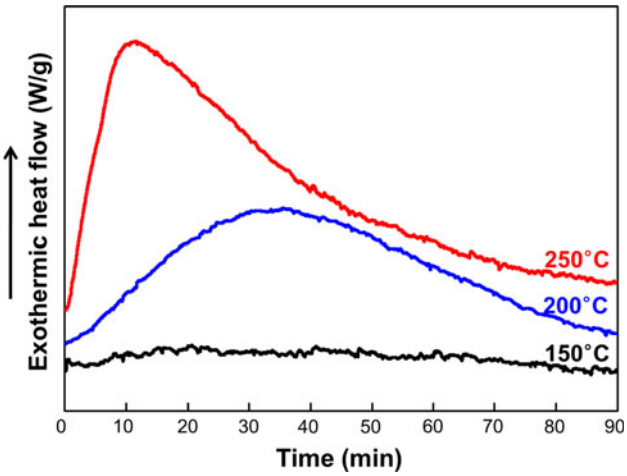

Fig. 4. DSC thermal profiles of isothermal conditions at 150°C, 200°C, and 250°C.

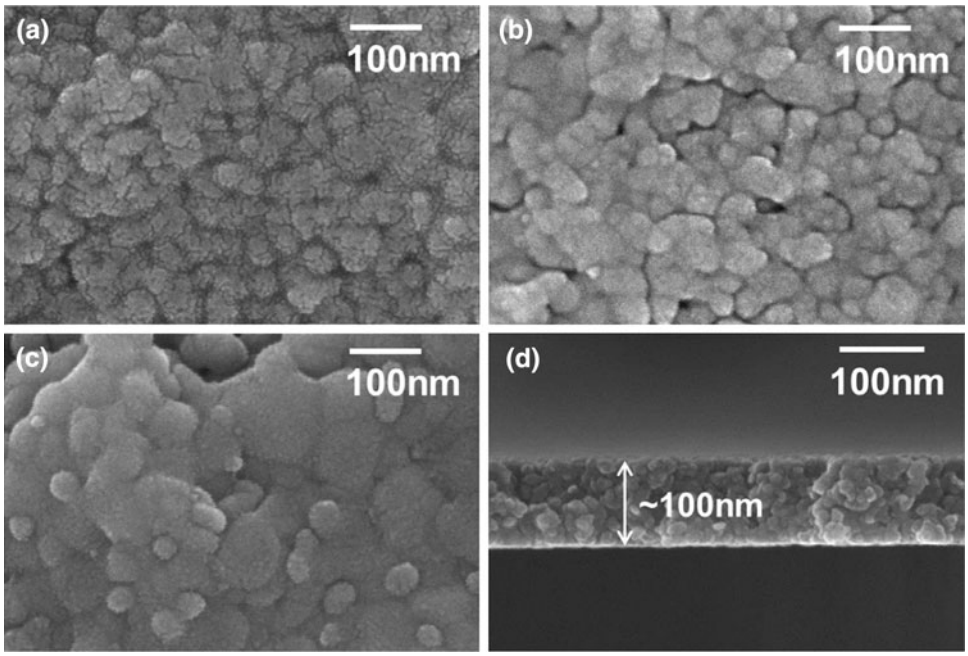

Fig. 5. SEM images of the surface morphology after 20 min of heating at (a) 150°C, (b) 200°C, and (c) 250°C. (d) Vertical section of the conductive films sintered at 200°C on Si wafer.

suitable for use in ink of hydrophobic nature.[22–24] Proper surface treatment can ensure that deposited films have uniform thickness. Conductive films generally have homogeneous electrical properties when their thickness is uniform, and as a result, they have a small deviation in terms of electrical resistivity. In fact, the surface treatment decreased the resistivity deviation from 30.01 $\mu\Omega$ cm to 0.559 $\mu\Omega$ cm. To further enhance the electrical properties, we eliminated the ligand shells disturbing the delivery of electrical signals by surrounding the metal nanoparticle. Generally, synthesis of metal nanoparticles has been conducted by using various additives such as organic surfactants, solvents, and reducing agents.[31–34] Several groups have also reported on the synthesis of metal nanoparticles with aliphatic amines as ligands for nanoparticles.[25,35,36] Moreover, the oleylamine used in this work is a well-known capping agent and a means of reducing equivalents.[35] Organoamines can passivate the surface of Ag nanoparticles and stabilize nanoparticles because of coordination of N atoms with Ag atoms originating from one-electron transfer from amines to Ag^+ ions at high temperature.[21]

Wakuda et al. suggested that dodecylamine capping shells, which increase the electrical resistivity, could be removed by dipping in methanol.[25–27] The same mechanism for removal of the capping shells was expected for oleylamine, which we used in this study as a kind of aliphatic amine, due to its similar structure to dodecylamine. Such removal may be influenced by the solubility of the aliphatic amine in methanol, which is reported to be higher than 90.3 wt.%. In this work, we also used methanol dipping treatment to remove the oleylamine cap from the surface of the nanoparticles.

Figure 6a shows TGA results for residual oleylamine at the surface under different conditions. For samples that underwent methanol dipping treatment, the residual oleylamine was reduced from 18.61 wt.% to 11.68 wt.%; furthermore, as shown in Fig. 6b, this reduction affected the electrical properties. The methanol dipping treatment reduced the electrical resistivity for all sintering temperatures. From the TGA results we could expect that the surfactant desorption temperature is related to the first stage of percolation transformation. The weight began to decrease at around 200°C regardless of methanol dipping treatment. This means that the residual oleylamine started to be desorbed and removed at this temperature. As shown in Figs. 5 and 6b, therefore, the surface morphology and electrical resistivity differed greatly with sintering temperatures. In the end, we obtained an electrical resistivity of 5.63 $\mu\Omega$ cm with sintering at 250°C. This value is close to that of bulk Ag material (1.59 $\mu\Omega$ cm).[16] The remaining difference in resistivity may be attributed to the presence of residual organic surfactants or incomplete sintering of the nanoparticles. In other words, the weight that is lost as the temperature increases corresponds to the residual oleylamine on the prepared metal nanoparticles. Thus, the reduction in residual oleylamine as a result of the methanol dipping treatment can reduce the total weight by around 7%. This behavior is closely related to the enhancement of electrical properties. Therefore, it is very likely that both the HMDS surface treatment and the methanol dipping treatment helped to diminish and stabilize the resistivity of the printed conductive film.

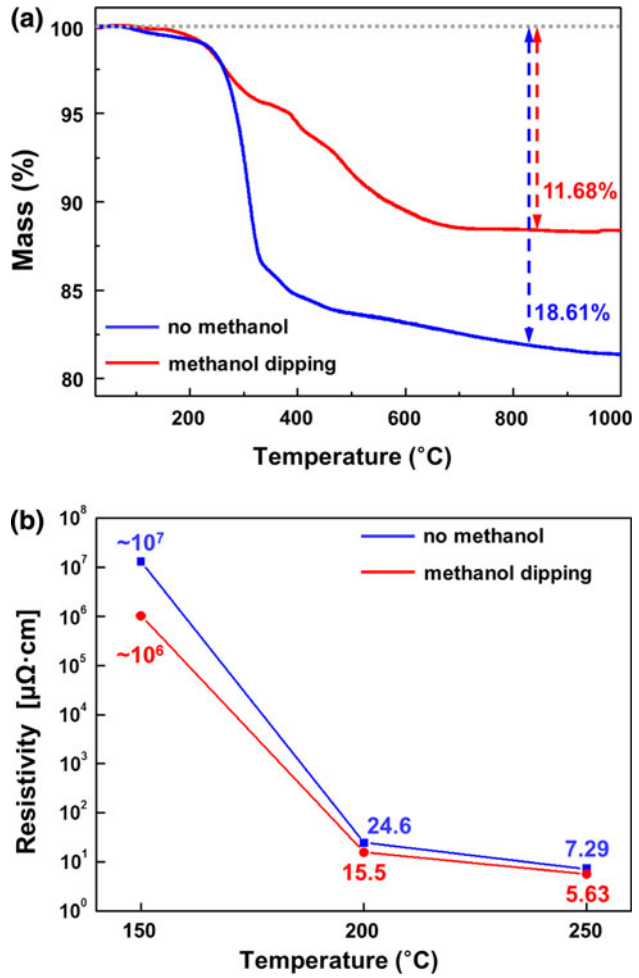

Fig. 6. (a) Weight loss of the conductive Ag ink measured by TGA. (b) Electrical resistivity of the Ag conductive films subjected to methanol dipping treatment as a function of sintering temperature.

CONCLUSIONS

We obtained various-sized Ag nanoparticles with diameter of 5.1 nm to 12.2 nm using a simple thermal decomposition, and 30 wt.% of Ag particles was mixed with HD solvent to make ink.

The electrical resistivity of conductive film printed by an inkjet printer using the Ag ink was measured as a function of the sintering temperature. It decreased with sintering temperature, but no difference was observed in terms of the size of the Ag nanoparticles in the ink.

HMDS treatment minimized the deviation of electrical properties, and methanol dipping treatment enhanced electrical properties. Due to the low processing temperature and low resistivity, the conductive ink made from Ag nanoparticles synthesized in this work provides a convenient way to fabricate electrical metal patterns in various printed electronics fields.

ACKNOWLEDGEMENTS

This research was supported by WCU (World Class University) program through the National Research Foundation of Korea funded by the Ministry of Education, Science, and Technology (R32-10051).

REFERENCES

1. M. Singh, H.M. Haverinen, P. Dhagat, and G.E. Jabbour, *Adv. Mater.* 22, 673 (2010).
2. B.J. de Gans, P.C. Duineveld, and U.S. Schubert, *Adv. Mater.* 16, 203 (2004).
3. D.J. Lee and J.H. Oh, *Thin Solid Films* 518, 6352 (2010).
4. S.H. Ko, H. Pan, C.P. Grigoropoulos, C.K. Luscombe, J.M.J. Frechet, and D. Poulikakos, *Nanotechnology* 18, 345202 (2007).
5. J. Park, D.J. Lee, S.J. Kim, and J.H. Oh, *J. Micromech. Microeng.* 19, 095021 (2009).

6. H.M. Dong, W.W. Carr, and J.F. Morris, *Phys. Fluids* 18, 072102 (2006).
7. P. Calvert, *Chem. Mater.* 13, 3299 (2001).
8. S. Sivaramakrishnan, P.J. Chia, Y.C. Yeo, L.L. Chua, and P.K.H. Ho, *Nat. Mater.* 6, 149 (2007).
9. J. Park, J. Joo, S.G. Kwon, Y. Jang, and T. Hyeon, *Angew. Chem. Int. Ed.* 46, 4630 (2007).
10. S.L. Lai, J.Y. Guo, V. Petrova, G. Ramanath, and L.H. Allen, *Phys. Rev. Lett.* 77, 99 (1996).
11. K. Dick, T. Dhanasekaran, Z.Y. Zhang, and D. Meisel, *J. Am. Chem. Soc.* 124, 2312 (2002).
12. Q. Jiang, S. Zhang, and M. Zhao, *Mater. Chem. Phys.* 82, 225 (2003).
13. T. Castro, R. Reifenberger, E. Choi, and R.P. Andres, *Phys. Rev. B* 42, 8548 (1990).
14. Y.H. Jo, J.C. Park, J.U. Bang, H. Song, and H.M. Lee, *J. Nanosci. Nanotechnol.* 11, 1037 (2011).
15. J.R. Greer and R.A. Street, *J. Appl. Phys.* 101, 103529 (2007).
16. J. Perelaer, A.W.M. de Laat, C.E. Hendriks, and U.S. Schubert, *J. Mater. Chem.* 18, 3209 (2008).
17. B.T. Anto, S. Sivaramakrishnan, L.L. Chua, and P.K.H. Ho, *Adv. Funct. Mater.* 20, 296 (2010).
18. S. Sivaramakrishnan, B.T. Anto, and P.K.H. Ho, *Appl. Phys. Lett.* 94, 091909 (2009).
19. K.S. Moon, H. Dong, R. Maric, S. Pothukuchi, A. Hunt, Y. Li, and C.P. Wong, *J. Electron. Mater.* 34, 168 (2005).
20. D. Kim and J. Moon, *Electrochem. Solid State Lett.* 8, J30 (2005).
21. M. Chen, Y.G. Feng, X. Wang, T.C. Li, J.Y. Zhang, and D.J. Qian, *Langmuir* 23, 5296 (2007).
22. M. Loughran, S.W. Tsai, K. Yokoyama, and I. Karube, *Curr. Appl. Phys.* 3, 495 (2003).
23. J.M. Kisler, M.L. Gee, G.W. Stevens, and A.J. O'Connor, *Chem. Mat.* 15, 619 (2003).
24. W. Ma, G. Li, Y. Zohar, and M. Wong, *Sens. Actuator A Phys.* 111, 63 (2004).
25. D. Wakuda, K.S. Kim, and K. Suganuma, *IEEE Trans. Compon. Packag. Technol.* 32, 627 (2009).
26. D. Wakuda, K.S. Kim, and K. Suganuma, *Scr. Mater.* 59, 649 (2008).
27. D. Wakuda, M. Hatamura, and K. Suganuma, *Chem. Phys. Lett.* 441, 305 (2007).
28. V. Pekkanen, M. Mantysalo, K. Kaija, P. Mansikkamaki, E. Kunnari, K. Laine, J. Niittynen, S. Koskinen, E. Halonen, and U. Caglar, *Microelectron. Eng.* 87, 2382 (2010).
29. A.L. Dearden, P.J. Smith, D.Y. Shin, N. Reis, B. Derby, and P. O'Brien, *Macromol. Rapid Commun.* 26, 315 (2005).
30. H.H. Lee, K.S. Chou, and K.C. Huang, *Nanotechnology* 16, 2436 (2005).
31. Y.H. Jo, I. Jung, C.S. Choi, I. Kim, and H.M. Lee, *Nanotechnology* 22, 225701 (2011).
32. S. Komarneni, D. Li, B. Newalkar, H. Katsuki, and A.S. Bhalla, *Langmuir* 18, 5959 (2002).
33. S. Ayyappan, R.S. Gopalan, G.N. Subbanna, and C.N.R. Rao, *J. Mater. Res.* 12, 398 (1997).
34. M.P. Mallin and C.J. Murphy, *Nano Lett.* 2, 1235 (2002).
35. H. Hiramatsu and F.E. Osterloh, *Chem. Mater.* 16, 2509 (2004).
36. N.R. Jana and X. Peng, *J. Am. Chem. Soc.* 125, 14280 (2003).